

# Collision Probability Forecasting using a Monte Carlo Simulation

Matthew Duncan  
*SpaceNav*

Joshua Wysack  
*SpaceNav*

Joseph Frisbee  
*United Space Alliance*

Space Situational Awareness is defined as the knowledge and characterization of all aspects of space. SSA is now a fundamental and critical component of space operations. Increased dependence on our space assets has in turn led to a greater need for accurate, near real-time knowledge of all space activities. With the continued growth of the orbital debris population, high-risk conjunction events are occurring more often. Consequently, satellite operators are performing collision avoidance maneuvers more frequently. Since any type of maneuver expends fuel and reduces the operational lifetime of the spacecraft, using fuel to perform collision avoidance maneuvers often times leads to a difficult trade between sufficiently reducing the risk while satisfying the operational needs of the mission. Thus the need for new, more sophisticated collision risk management and collision avoidance methods must be implemented. This paper presents the details of a method to forecasting how the collision probability evolves during an event. We examine various conjunction event scenarios and numerically demonstrate the utility of this approach in typical event scenarios. We explore the utility of a probability-based track scenario simulation that models expected tracking data frequency as the tasking levels are increased. The resulting orbital uncertainty is subsequently used in the forecasting algorithm.

## 1. INTRODUCTION

Space Situational Awareness (SSA) is defined as the knowledge and characterization of all aspects of space. SSA is now a fundamental and critical component of space operations. Increased dependence on our space assets has in turn lead to a greater need for accurate, near real-time knowledge of all space activities. With the growth of the orbital debris population, satellite operators are performing collision avoidance maneuvers more frequently. Frequent maneuver execution expends fuel and reduces the operational lifetime of the spacecraft. Thus the need for new, more sophisticated collision threat characterization methods must be implemented.

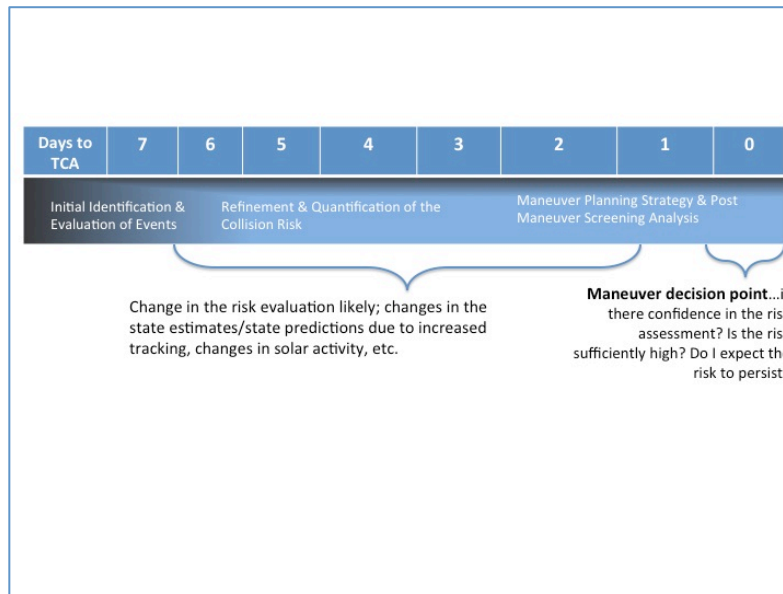
The collision probability metric is used operationally to quantify the collision risk. The collision probability is typically calculated days into the future, so that high risk and potential high risk conjunction events are identified early enough to develop an appropriate course of action.. As the time horizon to the conjunction event is reduced, the collision probability changes. A significant change in the collision probability will change the satellite mission stakeholder's course of action. So constructing a method for estimating how the collision probability will evolve improves operations by providing satellite operators with a new piece of information, namely an estimate or 'forecast' of how the risk will change as time to the event is reduced. Collision probability forecasting is a predictive process where the future risk of a conjunction event is estimated. The method utilizes a Monte Carlo simulation that produces a likelihood distribution for a given collision threshold. Using known state and state uncertainty information, the simulation generates a set possible trajectories for a given space object pair. Each new trajectory produces unique event geometry at the time of close approach. Given state uncertainty information for both objects, a collision probability value can be computed for every trail. This yields a collision probability distribution given known, predicted uncertainty.

## 2. DAILY PROCESSING OF CONJUNCTION EVENT DATA

Satellite close approach predictions are produced daily by Air Force personnel at the Joint Space Operations Center (JSpOC) at Vandenberg AFB. If two objects are predicted to come within some separation threshold, JSpOC personnel will issue a warning report and notify the appropriate satellite operator. The JSpOC provides various data products to the operator so that the collision risk can be established. Quantifying the collision threat typically involves include computing the collision probability, estimating how the probability will evolve, and trending various event parameters to establish consistency among solutions.

Once a high-risk conjunction event is identified, various avoidance scenarios are generated. Clearly the maneuver planning process must produce an orbit change that reduces the collision risk, while still meeting various operational constraints. Common operational constraints include restrictions on: maneuver magnitude, maneuver direction, and the time of day when the maneuver can be executed. The final constraint is to ensure that the selected maneuver does not introduce any new high-risk events after the maneuver is performed.

**Figure 1: Notional CA Event Timeline**



The operational challenge is to find the right balance between reacting too early to a high-risk event, while still remaining in a position to plan and execute an avoidance maneuver at an operationally favorable point in time. If the current risk is high, the risk will most likely drop as the time to the close approach point is reduced. However, the risk may not drop to an acceptable level by the time a maneuver decision has to be made. Conversely, if the current risk is low, the future risk *could* increase as the event evolves. In either case, the spacecraft operator is forced into a situation where he must actively monitor the event all the way to the maneuver decision point. The goal of this research is to reduce the operational effort expended on the temporary false positives, while at the same time identifying likely risky events prior to them being characterized as high risk. Additionally, can we reliably identify an operationally significant fraction of close approach events where this technique is useful.

### 3. TYPICAL BEHAVIOR/EVOLUTION OF THE COLLISION PROBABILITY – APPROACHES & CHALLENGES FOR DECISION MAKING

The collision probability is the primary measure of risk for operational spacecraft. As noted in Section 2, the collision risk is estimated several days into the future, utilizing predictive state and state uncertainty information at a future close approach point in time. Several algorithms exist for computing the collision probability, including probability via Monte Carlo simulation and various numerical methods.

#### 3.1 Numerical Method for Computing Collision Risk

Most conjunction events occur at high relative velocities. The two objects are in close proximity to one another for a short amount of time for such events. This fact makes it possible to approximate the relative motion between the two objects as linear over the encounter time. The short encounter time also allows for the assumption that the position covariance can be taken as constant for the duration of the event, and the problem becomes a 2-dimensional problem. At the close approach point, a conjunction plane is formed, which is orthogonal to the relative velocity vector at TCA.

The projection of the combined covariance and the keep-out region onto the conjunction plane are used to form the 2-dimensional probability density function. The conjunction coordinates are formed by,

$$\begin{aligned}\hat{r} &= \frac{\hat{r}_1 - \hat{r}_2}{|\hat{r}_1 - \hat{r}_2|} \\ \hat{v} &= \frac{\hat{v}_1 - \hat{v}_2}{|\hat{v}_1 - \hat{v}_2|} \\ \hat{z} &= \hat{r} \times \hat{v}\end{aligned}$$

These unit vectors form the rows of a transformation matrix needed to place the relative position and combined covariance into the conjunction frame,

$$M = \begin{bmatrix} \hat{r} \\ \hat{v} \\ \hat{z} \end{bmatrix}.$$

The required transformations are then made through matrix multiplication,

$$\vec{\rho}_{conj} = M \vec{\rho}$$

and

$$C_{comb} = M(C_1 + C_2)M^T.$$

These two parameters are then reduced to their projections in the conjunction plane,

$$\tilde{\rho}_{conj} = \begin{bmatrix} \rho_{conj}(1) \\ \rho_{conj}(3) \end{bmatrix} = \begin{bmatrix} x \\ z \end{bmatrix}$$

and

$$C_{comb} = \begin{bmatrix} C_{comb}(1,1) & C_{comb}(1,3) \\ C_{comb}(3,1) & C_{comb}(3,3) \end{bmatrix}.$$

The keep-out region is defined to be a circle with radius  $HBR$ . The resulting  $P_c$  integral is expressed as,

$$P_c = \frac{1}{2\pi\sqrt{|C|}} \iint_A e^{-\frac{1}{2}\tilde{\rho}_{conj}^T C_{comb}^{-1} \tilde{\rho}_{conj}} dx \square dz.$$

The limits of integration for variables  $x$  and  $z$  are,

$$\begin{aligned}-\sqrt{HBR^2 - z^2} &\leq x \leq \sqrt{HBR^2 - z^2} \\ -HBR &\leq z \leq HBR\end{aligned}$$

### 3.2 Typical Conjunction Event Behavior

The ‘typical’ evolution of the collision probability for a time series of updates is shown below. Each point in the figure below is a specific solution for that day, where state and state uncertainty information is propagated to the close approach point. So each point represents a new solution for the same conjunction event. The time series behavior is to be expected, the risk starts out to be relatively high. As the time to the close approach event is reduced, the risk rises and passes through a peak, then drops. Although in this case the risk was *eventually* not high enough to warrant a collision avoidance maneuver, the risk did get high enough early on so that resources were assigned to analyze the event in detail, and even examine avoidance maneuver options. The behavior of this temporary ‘false positive’ event is what we are statistically forecasting as the evolution of the event develops.

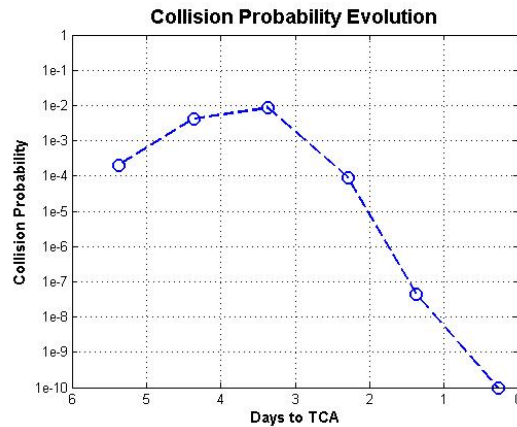
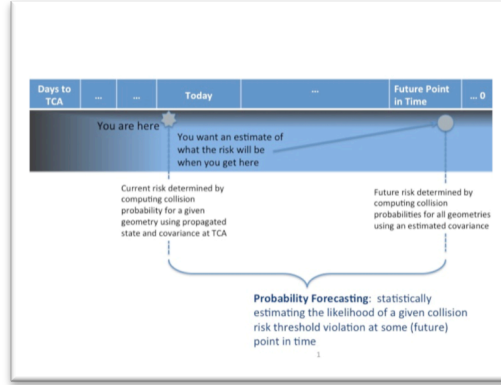


Figure 2. Typical evolution of collision probability

### 3.2 Forecasting Introduction

The ability to estimate the future risk at some future decision point would significantly improve operations. Spacecraft in Low Earth Orbit [LEO] routinely come close to cataloged objects where the collision risk is significant [3]. Since the collision probability is computed several days prior to the time of closest approach, the probability value will change leading up to the close approach point. Often times the observed change in the probability value is a reduction by orders of magnitude. The primary reason the collision probability value drops as the time is reduced is due to improved [i.e. reduced] state errors. Other contributing factors to the change in the collision probability are: new tracking data and atmospheric density changes [and thus a change to the estimated state]. So given a current estimate of the risk, we wish to estimate what the risk will be at some future point in time. Or said differently, for a given risk threshold, can I estimate the likelihood of violating that threshold at a some future time.



## 4. FORECASTING ALGORITHMS

### 4.1 Forecasting Via Direct Method

With current close approach data and an estimate of a future error covariance matrix at the time of closest approach it is reasonably possible, in some cases, to directly calculate the risk of a future solution violating a collision probability level (threshold). Speaking in terms of the relative state and position error in the collision plane, the current solution represents the distribution of possible locations of the true position with respect to the currently estimated position. However, the current position uncertainty may also be interpreted as a description of the distribution of possible future position estimates. The predicted covariance may then be interpreted as describing the distribution of the true position with respect to any realization of a future position estimate. The Gaussian probability density function (pdf) describing the location of the true position with respect to the unknown future position realization is then written as:

$$f(\mu_t, \mu_f) = \frac{e^{-\frac{1}{2}[\mu_t - \mu_f]^T C_f^{-1} [\mu_t - \mu_f]}}{2 * \pi \sqrt{\|C_f\|}} \quad (1)$$

(Subscripts  $f$  and  $t$  correspond to future value and true value respectively.)

Integration of this pdf with respect to true conjunction plane miss position  $m_t$  may be performed over the at risk area defined by the hard body radius (HBR). The result is the collision probability,  $P_c$ .

$$P_c = \int_{A_{HBR}} f(\mu_t, \mu_f) dA \quad (2)$$

This equation gives  $P_c$  as a function of the unknown future position,  $\mu_f$ . Generally, a closed form solution is not possible. However, it is however always possible to perform at least one analytic integration. The next step is to realize that if we are interested in the probability that some threshold will be violated in the future, then the left hand side of the  $P_c$  equation is known. So for instance, if a maneuver threshold of  $P_c = 10^{-4}$  is of interest then equation 2 represents an implicit expression describing the locus of points satisfying the equality. This set of points is that for which the estimated future position error covariance matrix, if located at any point on that locus, would yield a collision probability of  $10^{-4}$ . In order to perform a direct computation of the likelihood of a future estimate exceeding a given probability limit it is necessary to obtain at least a reasonable estimate of a more explicit description of this locus of points. One way is to

pick one component of the unknown miss position,  $\mu_f$  and then iterate on the other until the equality is acceptably satisfied. This procedure is repeated until enough point pairs have been determined to see if the locus is easily approximated by some simple function such as an ellipse. There are some commercially available software packages that plot two variable implicit functions. If such a plot package is used and appears to indicate the locus is approximately elliptical then only the two semi axes need to be estimated. This will be sufficient to define the locus. In order to make the locus description as simple as possible, the rotation of the data into the principal axis frame of the predicted future error covariance matrix is usually necessary.

Once the locus expression is available the final step is conducted. This step is to again use the current miss position and covariance matrix data (rotated into the future covariance principal axis frame) to compute a probability. In this case the area of interest is that bounded by the probability locus of interest rather than the usual HBR area. A simple, unitless, example follows with data chosen for simplicity to illustrate the idea.

$$\mu_c = [1000 \quad 200] \quad C_c = \begin{bmatrix} 750^2 & 0 \\ 0 & 150^2 \end{bmatrix} \quad C_f = \begin{bmatrix} 100^2 & 0 \\ 0 & 75^2 \end{bmatrix} \quad (3)$$

Assuming an HBR of 20, the Figure 3 illustrates this data and the boundary locus (using implicit function plotting).

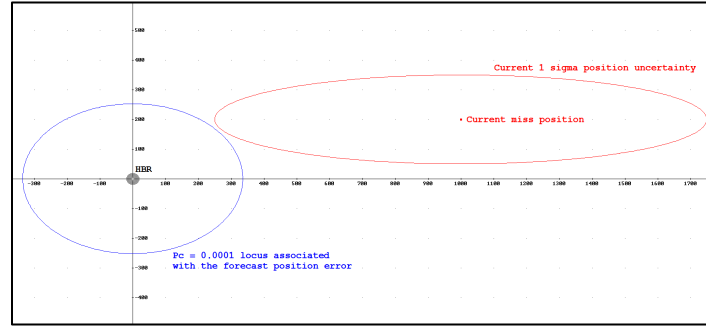


Figure 3. Example of current miss and uncertainty along with a forecast risk level boundary

From this figure and equation 2 it may be determined that the semi major and semi minor axes of the blue  $P_c = 10^{-4}$  boundary are approximately 335.49 and 252.58 respectively. In this case, a simple ellipse defined by these values is practically indistinguishable from the blue boundary line and so treating the boundary as an ellipse is reasonable. Using this approximation for the boundary, and integrating the pdf, defined by the current data, over the area inside this boundary will yield the probability  $P(P_c \geq 10^{-4}) \approx 0.074$ . The current data and given HBR provide a current collision risk estimate of  $P_c \approx 0.0003$ . For this data then, the current risk estimate exceeds a possible  $10^{-4}$  threshold but the likelihood of violating that same threshold in the future is low.

The ease with which this technique may be applied is related both to the ability to determine the locus of points defined by the implicit relationship in equation 2 and to then approximate that locus by a simple expression. One alternative to this last step is to define upper and lower boundary ellipses, or even rectangular boxes. Such upper and lower boundaries would bracket the risk of a future risk level violation. A last point is that by setting the unknown position components in equation 2 equal to zero, it is possible to determine the maximum collision probability associated with the forecast error covariance matrix. In the example here  $(P_c)_{\max}$  is approximate 0.026. This zero miss  $P_c$  indicates the maximum possible collision probability and so serves as an upper limit to various risk levels that might be analyzed using equation (2) in the implicit function fashion.

## 4.2 Forecasting Via Monte Carlo Simulation

A Monte Carlo simulation uses the statistical representation of the object states to simulate the conjunction event over a large number of trials. The possible trajectories of the objects is determined by sampling their

positions over the covariance using the latest state uncertainty information. This technique is similar to the technique used to compute the  $P_c$  via a Monte Carlo simulation. The forecasting algorithm then takes this a step further by calculating a  $P_c$  value for each Monte Carlo trial. The 2D numerical method is used for the  $P_c$  calculation. A predicted covariance is used in the  $P_c$  calculation that reflects the state error at the forecast epoch. Thus, the algorithm is taking into account the possible variations in the relative positions between the objects and the reduction in covariance size that will occur for epochs closer to TCA. The result is a distribution of  $P_c$  values. Figure 4 shows a sample distribution with the  $P_c$  values binned by order of magnitude. A useful metric is to determine the number of  $P_c$  values that violate a chosen  $P_c$  threshold.

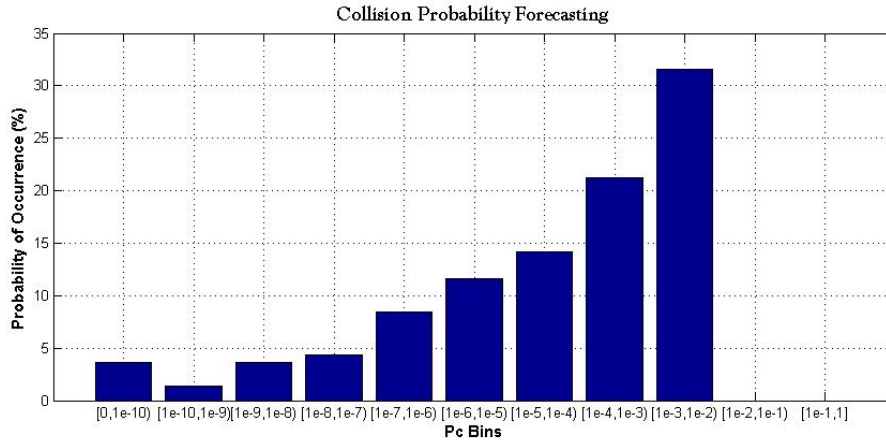


Figure 4. Sample  $P_c$  distribution from the Monte Carlo forecasting simulation

The algorithm for the  $P_c$  forecasting method is presented. The following definitions will be utilized in the algorithm,

- *Current epoch* – the epoch from which the forecast is made; e.g., a one-day forecast would make predictions one day past the baseline time
- *Forecast epoch* – the epoch at which the forecast is made
- *Forecast  $P_c$*  –  $P_c$  values calculated at the forecast time using the  $P_c$  forecasting method

The required inputs are state and covariance data for two objects with a predicted close approach  $n$  days into the future and a predictive covariance matrix for each object. State data is obtained from the latest orbit determination and then propagated to TCA. The predictive covariance can be obtained from a covariance time history file that reflects the correct propagation time. The steps of the Monte Carlo simulation are as follows:

1. Collect state and covariance data for both objects at the baseline time.
2. Form predictive covariance for each object in object-centered RIC frame that reflects uncertainty growth from forecast time to TCA
  - Forecast covariance can come from time history files, or
  - propagated VCM covariance
3. *Perform Monte Carlo simulation* – For  $i = 1:N$
4. Form perturbed trajectories by perturbing the state of each object according to its covariance
  - Utilize state & covariance at baseline time
5. Find the point of close approach & TCA for each set of perturbed trajectories
6. Align forecast covariances to perturbed states at TCA by rotating from object-centered RIC to ECI J2000
7. Calculate 2D  $P_c$  using perturbed states and forecast covariances
8. *End Monte Carlo simulation*

## 5. CASE STUDIES

Examination of 5 different Low Earth Orbit conjunction events were considered in our study. We post-process event data to see how well both the Direct Method and the Monte Carlo simulation perform. Event data comes from orbit determination updates of both objects. The state and state uncertainty are then propagated to TCA. Table 1 provides a summary of the case study events with a description of the event and how the forecasting algorithms performed.

Table 1. Summary of the conjunction event details and forecasting results for each case

Case	Event Description	Forecasting Outcome
LEO #1	Typical behavior of Pc evolution where risk starts out high and then drops as the time to TCA is reduced	Correctly predicts that there is a low chance of a high Pc at TCA
LEO #2	Typical behavior of Pc evolution where risk starts out high and then drops as the time to TCA is reduced	Correctly predicts that there is a low chance of a high Pc at TCA
LEO #3	High risk for the lifetime of the event that would warrant consideration of a risk mitigation maneuver	Provides evidence that the risk will remain high at TCA
LEO #4	Typical behavior of Pc evolution where risk starts out high and then drops as the time to TCA is reduced	Correctly predicts that there is a low chance of a high Pc at TCA
LEO #5	The risk evolves from low to high during the lifetime of the event	Forecasts to TCA indicate that risk will increase, but is not likely to violate a maneuver risk threshold

Section 5.1 provides a description of the events and the forecast results. The results are from the Monte Carlo simulation. Section 5.2 provides a comparison of output from the two forecasting algorithms.

### 5.1 Case Study Results

For each conjunction event the evolution of the risk will be shown for each orbit update. This data is from the actual orbit data and represent the risk (in terms of Pc and miss distance) at the time the data was received.

Forecasting results are presented as the likelihood of violating a set Pc threshold. The Pc threshold was set to  $1e-4$  to coincide with a typical value used by satellite operators as a risk threshold to perform a risk mitigation maneuver. Forecasts can be performed for any forecast epoch in the future. Here we will present results for forecasts to the TCA.

#### LEO #1 Event – Background

This event is a typical close approach between two objects in LEO orbit. From the outset, the risk was high; with Pc greater than the Pc threshold used in this study of  $1e-4$ . As can be seen in the Pc evolution plot in the Figure 5, the Pc remained at or above the Pc threshold until an update at TCA – 1.4 days. As the event evolved the Pc dropped down to a level where there is was no longer a threat of collision.



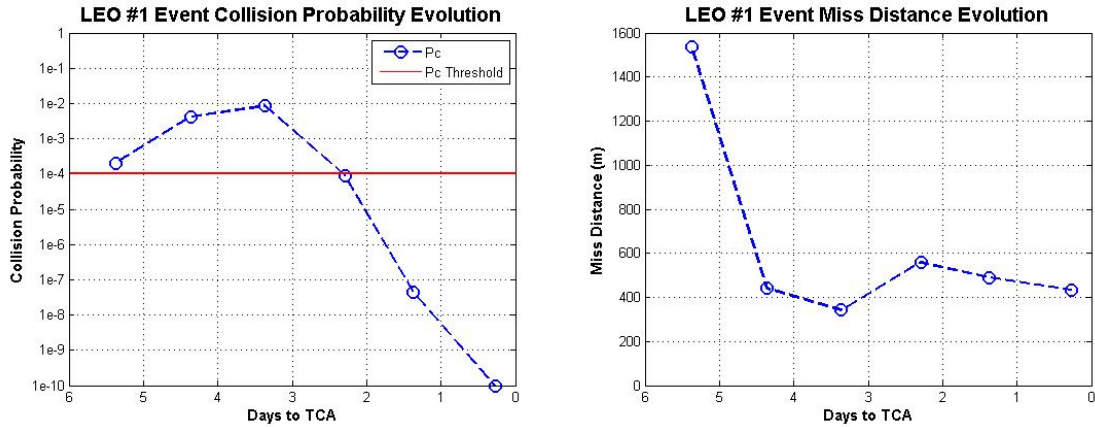


Figure 5. Collision probability and miss distance evolution for the LEO #1 event

### LEO #1 Event – Forecast Results

This event would be classified as high risk and would likely require work for maneuver planning preparation. The forecasting algorithm can provide useful information to determine whether maneuver planning should occur and whether a planned maneuver will be executed.

Figure 6 provides results for a forecast to TCA performed at each orbit update. For this study we use the time of the last orbit update as a proxy for the TCA so that the forecast results can be compared against a point in time in which data is available. The data is the probability that the Pc will be greater than 1e-4 at TCA. The first forecast performed at TCA – 5.4 days suggests that the risk will not be high at TCA. The likelihood of high risk at TCA goes up with the next two updates. The Pc calculated at TCA – 2.3 days provides the current risk to be at the Pc risk threshold (see Figure 5), while the forecast projects that there is only a 3.9% chance of the Pc staying at that level. That forecast is correct, as the Pc drops to zero over the next two updates.

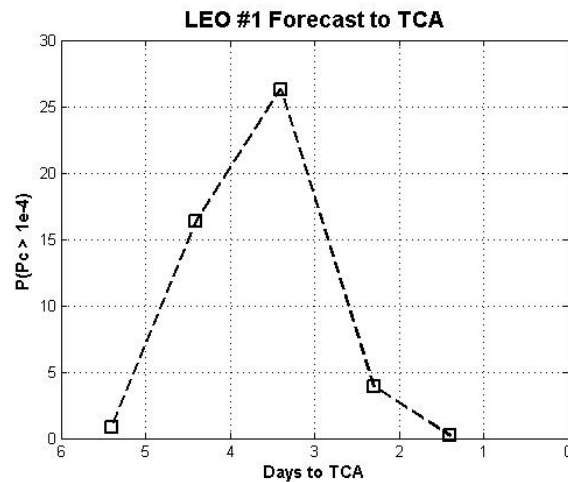


Figure 6. Evolution of results for forecasts to TCA for the LEO #1 event

### LEO #2 Event – Background

The evolution of this event is similar to the LEO #1 event. The  $P_c$  at the first orbit update was high even though the miss was 3542 m. At TCA – 3.4 days the predicted miss distance dropped down to 34 m. Subsequent orbit updates showed that the objects were actually predicted to be several kilometers apart. This resulted in a large drop in the  $P_c$  until it was effectively zero near TCA.

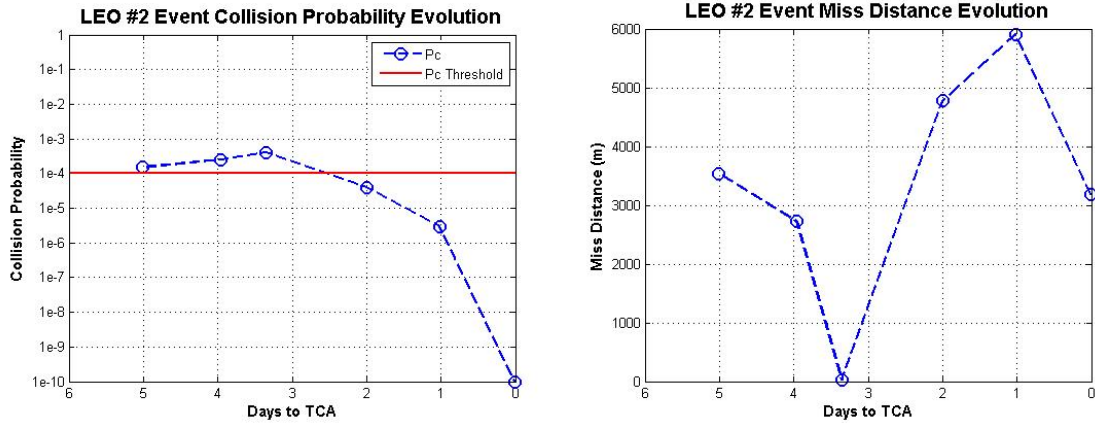


Figure 7. Collision probability and miss distance evolution for the LEO #2 event

### LEO #2 Event – Forecast Results

The forecast evolution for this event appears similar to that for the LEO #1 event, however, this case forecasts provides a clear indication that the risk will be below the  $P_c$  threshold at TCA. At TCA – 3.4 days the  $P_c$  is  $4.07 \times 10^{-4}$  and the miss distance is 34 m. Given this information the risk would be deemed high and the initial steps of risk mitigation maneuver planning would be begun. The forecast result at this time projects that there is less than a 5% chance that the  $P_c$  will be above the risk threshold at TCA. As in the first sample case, the forecast accurately predicts that the event is not a risk.

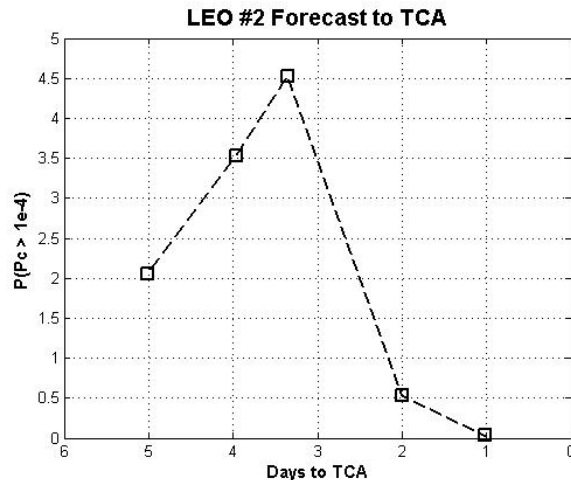


Figure 8. Evolution of results for forecasts to TCA for the LEO #2 event

### LEO #3 Event – Background

This event had high risk for the entire lifetime of the event. Despite a jump in the miss distance at TCA – 3.4 days, the  $P_c$  remained above  $1e-4$ . This is an example of a case where mission management would have to make a decision of whether a risk mitigation maneuver is warranted.

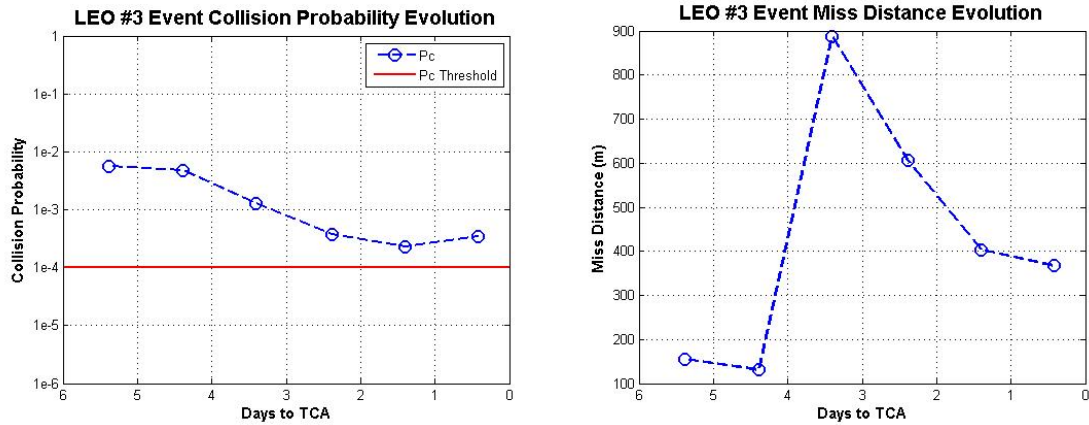


Figure 9. Collision probability and miss distance evolution for the LEO #3 event

### LEO #3 Event – Forecast Results

Given the consistent high risk of this event, the task for the forecasting algorithm is to provide indication that the risk will remain high at TCA. Figure 10 shows that the forecast results are fairly consistent in the likelihood that the  $P_c$  will be above  $1e-4$ . Though the forecast percentages stay below 50%, at TCA – 1.4 days the chance of the  $P_c$  being above the  $P_c$  threshold at TCA is a compelling piece of information when mission stakeholders are considering whether to perform an avoidance maneuver.

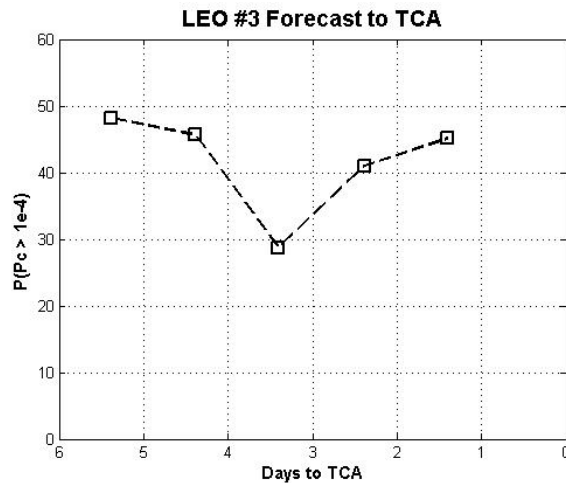


Figure 10. Evolution of results for forecasts to TCA for the LEO #3 event

### LEO #4 Event – Background

The evolution of this event is typical of many of those that are seen in satellite operations. The initial prediction was that the risk was high. The  $P_c$  remained above the  $P_c$  threshold until an orbit update at TCA – 3 days, at which point it dropped to a point that would not warrant a risk mitigation maneuver. As seen in Figure 11, in subsequent orbit updates the  $P_c$  dropped to zero.

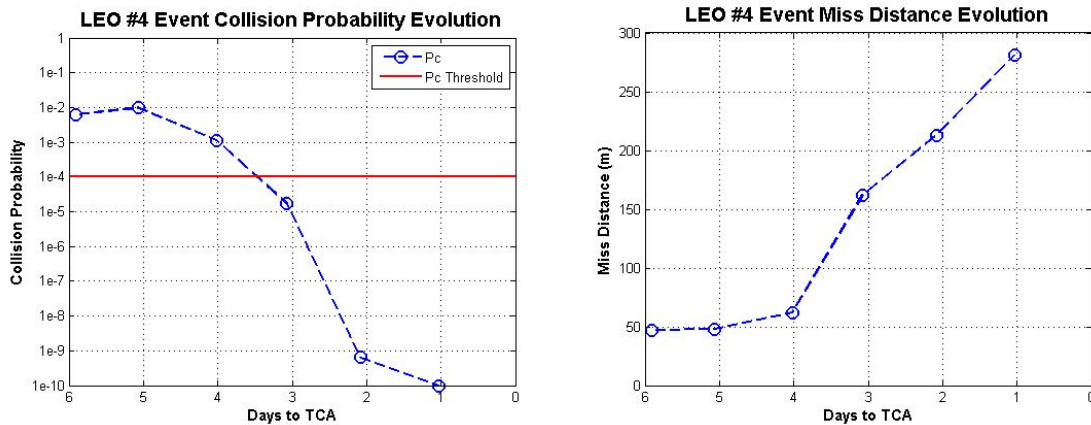


Figure 11. Collision probability and miss distance evolution for the LEO #4 event

### LEO #4 Event – Forecast Results

Once again the forecast algorithm works well for an event that goes from high risk to low risk as successive orbit updates are received. The initial forecasts do indicate that the risk may be high at TCA, but beginning at TCA – 3 days it is clear that the chance of a high risk event is low.

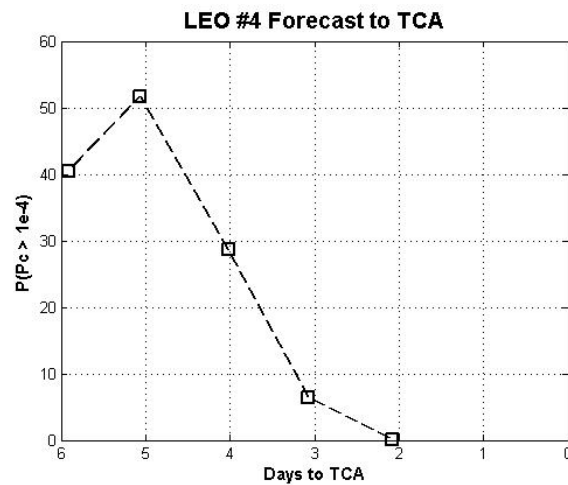


Figure 12. Evolution of results for forecasts to TCA for the LEO #4 event

### LEO #5 Event – Background

The miss distance for this event has a dramatic change during the course of the event lifetime. The first orbit update indicated that the objects were ~22 km apart. Even at this large miss distance, the  $P_c$  was not zero, though it did indicate low collision risk. With further orbit updates, the two objects were predicted to come closer together. This culminated in a final predicted miss distance of 84 m. The  $P_c$  rose beyond the  $1e-4$  threshold near the TCA – 2 day point, but then dropped lower near TCA. For this event the secondary object had poor tracking, which did not improve during the course of the event. The  $P_c$  and miss distance evolution are shown in Figures 13.

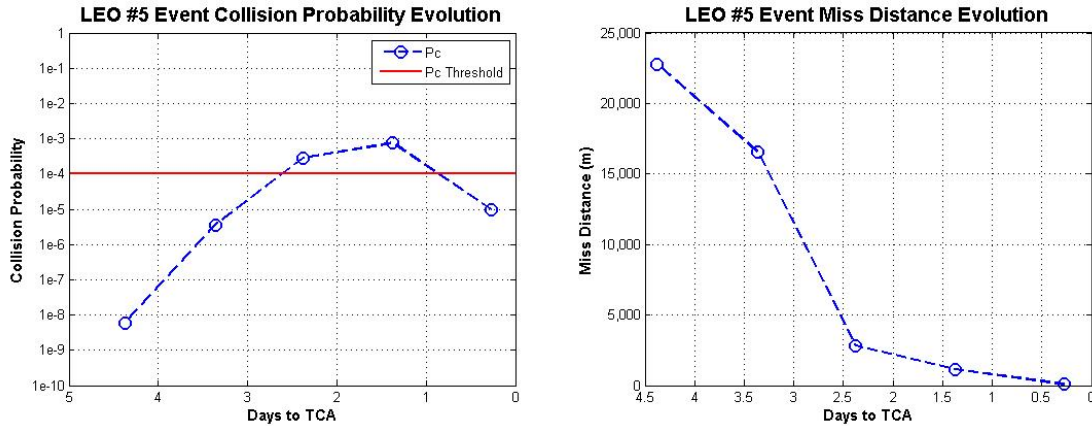


Figure 13. Collision probability and miss distance evolution for the LEO #5 event

### LEO #5 Event – Forecast Results

This is a stressing case for the forecasting algorithm. The secondary object had several orbit updates where the position changed on the order of 3-sigma in its uncertainty. Since the forecasting algorithm varies the position of the objects over their covariance at the current epoch, this 3-sigma change in miss is a case that is statistically unlikely to happen. This is reflected in the forecasting results shown in Figure 14. However the algorithm result did forecast a low probability that the  $P_c$  would be above the threshold at TCA, which turned out to be the case.

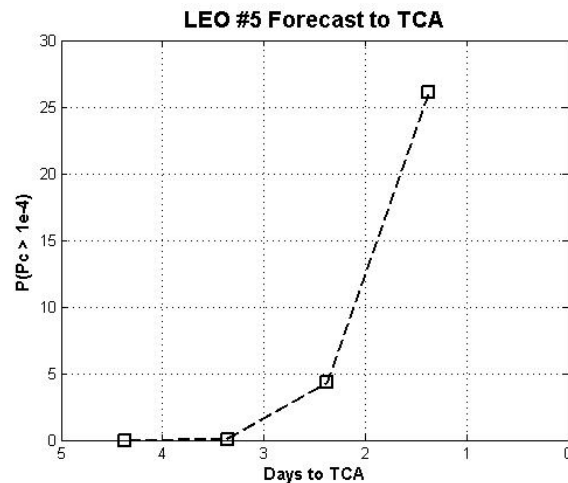


Figure 14. Evolution of results for forecasts to TCA for the LEO #5 event

## 5.2 Direct Method and the Monte Carlo simulation Comparison of Results

Both methods were run for a series of sample conjunction events to ensure that they achieved similar results. Table 2 provides a comparison of the forecast results for a sample case. As before, these are the probabilities that the  $P_c$  will be greater than  $1e-4$  at TCA. Results agreed very well in this case as they did for all other cases.

Table 2. Forecast results for the Direct Method and the Monte Carlo simulation

Current Epoch (Days to TCA)	Direct Method $P(P_c > 1e-4)$ at TCA (%)	Monte Carlo Simulation $P(P_c > 1e-4)$ at TCA (%)
5	17.4	17.1
4	25.7	25.4
3	39.8	39.8
2	59.3	58.0
1	75.4	74.2

## 6. OPERATIONAL UTILITY & CONSIDERATIONS

### 7. CONCLUSIONS & FUTURE WORK

Both the Monte Carlo simulation and direct method work well for the cases considered...in particular for sufficiently short forecast times

Future work to incorporate the likelihood of acquiring further tracking in future OD updates

Variation dependent upon likelihood of a sensor acquiring track data

Perform sensitivity analysis to determine how sensitive the forecast results are to the size of the predicted covariance

## 8. REFERENCES

- [1] A. Bleich, M. Duncan, and J. Wysack, "The Collision Risk Assessment & Risk Mitigation Process For the NPP & NPOESS Missions," AAS 09-375.
- [2] Newman, Lauri and Duncan, Matthew. "Establishment and Implementation of a Close Approach Evaluation and Avoidance Process for Earth Observing System Missions." AIAA/AAS Astrodynamics Specialist Conference Proceedings. 21-24 August 2006.
- [3] Newman, Lauri. "The NASA Robotic Conjunction Assessment Process: Overview and Operational Experiences." 59<sup>th</sup> International Astronautical Congress Conference Proceedings. 29 September – 3 October 2008.